

Robotic delivery of laser-induced breakdown spectroscopy for sensitive chlorine measurement in dry cask storage systems

D.G. Fobar^a, X. Xiao^{a,b,c}, M. Burger^{a,b,*}, S. Le Berre^c, A.T. Motta^c, I. Jovanovic^{a,b}

^a Department of Nuclear Engineering and Radiological Sciences, University of Michigan, Ann Arbor, MI, 48109, United States

^b Center for Ultrafast Optical Science, University of Michigan, Ann Arbor, MI, 48109, United States

^c Department of Mechanical and Nuclear Engineering, The Pennsylvania State University, University Park, PA, 16802, United States



ARTICLE INFO

Keywords:

Laser-induced breakdown spectroscopy (LIBS)
Optical fiber
Remote inspection
Double pulse
Chlorine

ABSTRACT

Chlorine-induced stress corrosion cracking is a degradation mechanism of concern for dry storage of used nuclear fuel. Remote detection of chlorine deposited on the stainless steel canister surface presents a challenge, since no direct line-of-sight is available. We demonstrate the design and use of double-pulse laser-induced breakdown spectroscopy installed on a robotic system for remote detection and measurement of the canister surface chlorine concentration. The system meets the stringent requirements of dry cask storage inspection environment, especially the constrained space. The externally located pulsed laser, spectroscopic instrumentation, and data acquisition setup were interfaced to a robotic delivery car using a pair of 25-m long optical fibers. We discuss the design and construction details of the chlorine detection system and its detection performance in both laboratory and field-deployable configurations. We show that chlorine concentrations as low as 10 mg/m² can be measured in field-compatible operations.

1. Introduction

Until geological disposal of spent nuclear fuel becomes available, spent nuclear fuel is stored on site in dry storage facilities, in which the spent fuel assemblies are enclosed in stainless steel canisters within a concrete overpack. Due to the unavailability of final disposal, the expected residence times of spent fuel in dry storage could be much longer than previously expected. This raises the possibility that slow developing degradation mechanisms could become of concern. One of these mechanisms is stress corrosion cracking of the metal in a marine environment, where salt deposition on the canister surface could assist crack propagation (Chu, 2013; Bryan and Enos, 2015). Thus it is necessary to assess the amount of salt (or chlorine) present on the surface of the canister after a long period of storage. It is highly desirable that such a measurement be performed remotely, in order to minimize the cost and time needed for inspection.

In this work we present a method for the direct measurement of chlorine (Cl) concentration levels on stainless-steel using a laser-induced breakdown spectroscopy (LIBS) (Miziolek et al., 2006; Noll, 2012; Cremers and Radziemski, 2013) system, which is fully integrated into a multi-sensor inspection system. LIBS is based on the principle that when a focused laser pulse of sufficient intensity strikes a target, a small surface layer of the material is ablated and ionized, forming a fast

expanding plasma. During the relaxation of this plasma, ions, atoms, and/or molecules at a later stage, emit photons of specific wavelengths that are characteristic of the atomic species present on the surface of the canister and ablated into the plasma. This allows the detection of materials deposited on surfaces, even in relatively small concentrations. Both chlorine and iron (the major constituent of the steel canister) exhibit prominent atomic spectral lines in the infrared spectral region (Kramida et al., 2017). In particular, the Cl I spectral line at 837.6 nm is especially useful for the purpose of chlorine detection. By combining the methods of emission spectroscopy and carefully developing calibration curves (Gornushkin et al., 1999; David and Omenetto, 2010), a quantitative relationship can be established between the chlorine spectral line intensity and its corresponding concentration on a stainless steel surface. This approach has been explored by several research groups (Wilsch et al., 2005; Gehlen et al., 2009; Eto and Fujii, 2016), which have all encountered the challenge associated with the high ionization potential of chlorine. In order to address this challenge and to enhance the signal-to-background ratio for the spectral line observed, we used the double-pulse (DP) LIBS technique (Benedetti et al., 2005; Babushok et al., 2006). DP lasers are now commercially available and are becoming increasingly more compact (Li et al., 2017). In the DP technique, the first pulse ablates the target, while the second effectively reheats the plasma, mainly via the inverse bremsstrahlung mechanism,

* Corresponding author. Department of Nuclear Engineering and Radiological Sciences, University of Michigan, Ann Arbor, MI, 48109, United States.
E-mail addresses: milosb@umich.edu (M. Burger), ijov@umich.edu (I. Jovanovic).

thus enhancing the signal. The DP method has already proven its success in the detection of chlorine on concrete surfaces (Labutin et al., 2013) and in an iron-oxide mixture (Pedarnig et al., 2014).

In the case of inspection of dry cask storage for used nuclear fuel, LIBS has to be compact and suitable for *in-situ* deployment. A multi-sensor robotic platform, dubbed the PRINSE (Proactive Robotic Inspection of Nuclear Storage Enclosures), has been developed to address a set of more comprehensive inspection requirements (Lissenden et al., 2016). The PRINSE system consists of a train that includes electromagnetic acoustic transducers, LIBS, and temperature and radiation sensors. This suite of sensors enable PRINSE to detect cracks, measure the concentrations of chlorine and other elements on the canister surface, and characterize the temperature and radiation field. Inside the payload area of the train car dedicated to LIBS, the optics is constrained to a height of 32 mm and a footprint of 100 mm × 80 mm. This spatial constraint poses a significant challenge in the engineering design of the LIBS delivery with commercial off-the-shelf optics. Additionally, since the robotic train is required to operate in a deep channel of a dry cask storage container that can only be accessed from its top, 25-m long optical fibers are used to deliver the laser pulse and collect and transport the light collected from the plasma radiation. In Fig. 1 we present the conceptual design and principle of operation of a fully portable, remotely delivered DP LIBS system capable of performing sensitive detection of trace elements on metal surfaces. We demonstrate its integration with the PRINSE multi-sensor robotic system and present the initial results of the determination of its detection limit for chlorine on stainless steel in a testbed that captures the relevant characteristics of dry cask storage systems.

2. Summary of feasibility study

Halogen elements can be challenging to detect via LIBS because their energy level distribution has many high-lying upper energy states. For example, the strongest resonance transitions of chlorine are in the vacuum ultraviolet spectral region, which is not suitable for LIBS measurements under typical ablation conditions due to absorption occurring in the atmosphere and in optical materials. However, the Cl I spectral line located at 837.6 nm is the most intense chlorine emission line outside the vacuum ultraviolet region, and has been shown to be readily detectable in LIBS. The limit of detection is typically in the tens of thousands of mg/l, but has been reduced significantly, by applying high incident laser energy (Wilsch et al., 2005; Gehlen et al., 2009; Tran et al., 2001; Burakov et al., 2007; Sugiyama et al., 2010), adopting helium buffer gas (Wilsch et al., 2005; Gehlen et al., 2009; Sugiyama et al., 2010), or using an additional excitation technique such as pulsed electric discharge (Burakov et al., 2007) and DP (Sugiyama et al., 2010; Labutin et al., 2014).

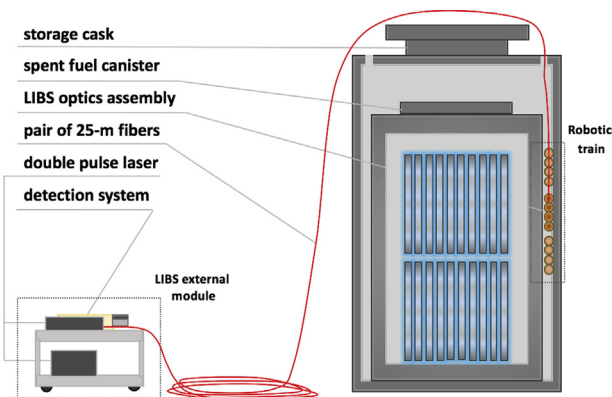


Fig. 1. Illustration of the design concept of a robotically delivered LIBS system for characterization of surface composition of the steel canister in dry cask storage.

The capability of LIBS to provide remote *in-situ* measurements of elemental concentrations is attractive for use in challenging environments such as dry cask storage containers. In addition to high temperature, another important aspect of the dry cask storage environment is the limited space and lack of direct line of sight of the inspected surface. These constraints can be overcome by fiber delivery of high-power laser pulses to the location of interest and the transport of collected optical emission from the plasma through the optical fiber. The bulky and temperature sensitive components of the LIBS system such as the laser, spectrometer, and fast-gated detector can be located outside the overpack. Additionally, optical fiber provides strong confinement of laser light, which shields the personnel from laser hazards and eliminates the possible effect of atmospheric turbulence on laser delivery and LIBS signal collection. The fiber probe can be carried by the robotic train, which eliminates the need for optical alignment along its path. Optical fibers show relatively high radiation tolerance in the near-infrared region (Saeki et al., 2014), and their composition can be further tailored to enhance radiation resistance (Girard et al., 2013; Nagasawa et al., 1984).

2.1. DP excitation in fiber-optic LIBS

The performance of fiber-optic LIBS is affected by several constraints that are not present in open-beam delivery, including the optical damage of the fiber that limits the peak power that can be delivered onto the sample surface, imperfect laser-fiber coupling that results in further reduction of peak power at the output of the fiber, intermodal dispersion that stretches the laser pulse after propagating through the fiber, and large beam divergence and limited focusability at the fiber output. These constraints limit the maximum achievable laser intensity necessary for observing chlorine emissions at low concentrations. In most prior successful “real world” applications of fiber-optic LIBS that require remote analysis to be made *in situ*, no special attention was paid to the halogen chlorine (Saeki et al., 2014; Davies et al., 1995; Cremers et al., 1995; Neuhauser et al., 2000; Rai et al., 2001; Whitehouse et al., 2001). The exception is the work of Eto and Fujii, who demonstrated the potential of detecting the Cl I emission (837.6 nm) at concentrations as low as 50 mg/m² using fiber-optic LIBS (Eto and Fujii, 2016). They used single-pulse excitation and a fiber length of 5 m. However, it remains desirable to further reduce the limit of detection and to conduct measurements over fiber distances exceeding 5 m.

In our recent work, the DP excitation technique was introduced in fiber-optic LIBS to improve its limit of detection for chlorine measurements (Xiao et al., 2018). By splitting a single laser pulse into two and delaying one of them to realize a DP configuration, more energy can be delivered through the optical fiber. In DP ablation a significant enhancement of the characteristic emission from plasma resulted due to a larger population of excited analyte atoms formed by reheating the preformed plasma. The enhanced material removal and increased atomized analyte atoms in the plasma volume also contribute to the enhancement of the characteristic emissions. An approximate 5-fold increase of the intensity of emission lines was achieved. This high emission intensity allowed the identification of the lines and quantification of the chlorine concentrations at levels as low as 5 mg/m² (Xiao et al., 2018). Furthermore, this increase of sensitivity was achieved concurrently with extending the fiber distance to 25 m, with possibility for future extension.

2.2. Laboratory testing overview

Initial laboratory tests were performed using a 10-ns, 10-Hz Nd:YAG laser (Quanta-Ray PRO-250-10, Spectra Physics). The fundamental wavelength of the Nd:YAG laser was used, since the signal-to-background ratio of the Cl I line induced by the 1064-nm laser pulse was experimentally determined to be much higher than that generated when using the second-harmonic (532 nm) wavelength. The energy of

1064-nm laser pulse that can be transmitted through the fiber is much higher than that of 532-nm pulse due to the lower photon energy, resulting in a higher damage threshold. The DP was formed by splitting the laser pulse into two pulses of equal energies, introducing a 40-ns delay between them by free-space propagation, and combining the temporally separated pulses into a DP sequence. Using a multimode fiber (FT1000EMT, Thorlabs) with a core diameter of 1 mm and transmission efficiency of 66%, it was possible to transmit 40 mJ per pulse. The plasma emission was collected at an angle of 45° with respect to the incident beam and subsequently diverted through a quartz fiber to be resolved by a Czerny-Turner spectrometer (iHR550, Horiba Jobin Yvon) and recorded by an ICCD camera (iStar 334T, Andor). With this fixed 40-ns interpulse delay setup, chlorine concentrations as low as 5 mg/m² could be measured. Using well-calibrated samples of predetermined concentrations, a calibration curve between concentration and recorded signal was obtained. In the calibration process, the chlorine concentration was calculated on the basis of the known quantity of NaCl used in sample preparation process (Xiao et al., 2018). This calculated concentration was quantitatively validated using ion chromatography (Xiao et al., 2017).

Further laboratory testing incorporated a portable DP Nd:YAG laser (Evergreen 70, Quantel) that combines two separate laser cavities to produce pulses at arbitrary delays, which are then combined into a single beam. The DP laser was operated at a pulse duration of 15 ns and a repetition rate of 10 Hz at its fundamental wavelength. A 7.3% broadening of pulse duration was measured after transmission through the 25-m long multimode fiber. A custom remote optical assembly was developed to deliver the high-power laser pulses from the fiber to the sample surface and to collimate the plasma emission back to a separate 25-m long fiber in a non-coaxial configuration (as discussed in more detail in later sections). The same spectral resolving system including the spectrometer and the ICCD camera was used (Xiao et al., 2018).

Parametric studies of the DP enhancement effect were performed in order to maximize the Cl I spectral emission. The magnitude of the enhancement is dependent on the interpulse separation in the DP sequence and the exact conditions of laser-plasma coupling (Babushok et al., 2006). Fig. 2 shows a series of measurements of the spectral region of interest, using a range of interpulse delays. As can be seen in Fig. 2, the maximum enhancement of the Cl I line was observed at an interpulse delay of 750 ns. We conducted more systematic studies, showing that in our configuration a 900-ns interpulse delay and a gate width of 2100 ns at a delay of 300 ns results in the optimal LIBS performance for the measurement of the chosen Cl I line (Fig. 3). The emission from the rapidly expanding plasma can be measured more

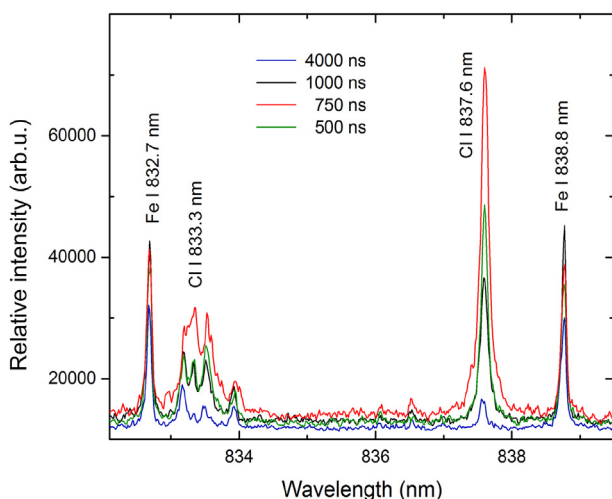


Fig. 2. Example measurement of the spectral region of interest showing chlorine and iron line profiles recorded at various interpulse delays.

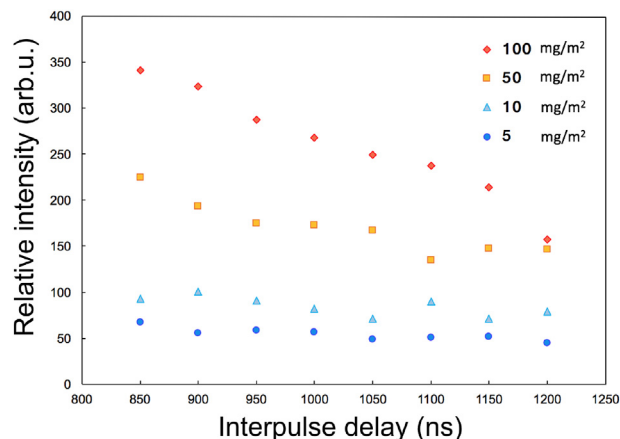


Fig. 3. Intensity of Cl I 837.6 nm spectral line as a function of interpulse delay for different chlorine concentrations at a fixed gate-width time of 2.1 μ s.

consistently with a long ICCD gate, which addresses the limited field of view provided by the compact remote optical system.

Quantification of chlorine surface concentrations in the range of 5–100 mg/m² was demonstrated for the first time recently (Xiao et al., 2018). These feasibility studies give confidence that fiber-optic LIBS in DP configuration can be used to measure chlorine concentrations as per the requirements of dry cask storage system inspection.

3. Technical design

The development of the PRINSE LIBS subsystem encompassed three major tasks. First, it was necessary to develop an optical system that allows for the detection of chlorine while not exceeding the allotted payload volume. Second, the final optical system had to be integrated with the train car. Third, the externally located components of the LIBS system (the laser source, fiber launch optics, spectrometer, and time-gated detector) needed to be packaged into a compact, mobile assembly that integrates with the PRINSE command and control network. Accomplishing the first task required multiple design iterations and experimentation, while the second task was highly dependent on the design of the PRINSE robotic system and the optical layout, both of which were concurrently developed. The third task could be carried out largely independently, but included important considerations, such as environmental conditions and laser safety.

3.1. Optical design

Laser delivery and the collection of surface plasma emission are implemented as two separate optical systems and are interfaced to the external LIBS module via two optical fibers. Combining the two in a coaxial configuration employing a single optical fiber was considered, but not used due to challenges of efficiently coupling and collimating light of different wavelengths, with different divergences, and with some differences in the source location (e.g. the optimal location for plasma light collection is slightly above the sample surface). The two separate optical paths are arranged in a single holder designed to be 3D-printed. In order to maintain critical optical alignments, the collection optics are constrained in a single tube and adjusted as an assembly. This allows for a single point of adjustment for overlapping the focal spots of the two optical paths.

3.1.1. Laser delivery

Two collinear and orthogonally polarized 1064-nm laser pulses are generated using a commercial double-pulse Q-switched Nd:YAG laser (Quantel Evergreen 70). Each sample location receives a sequence of three double pulses, and the sequences are conducted at the optimal

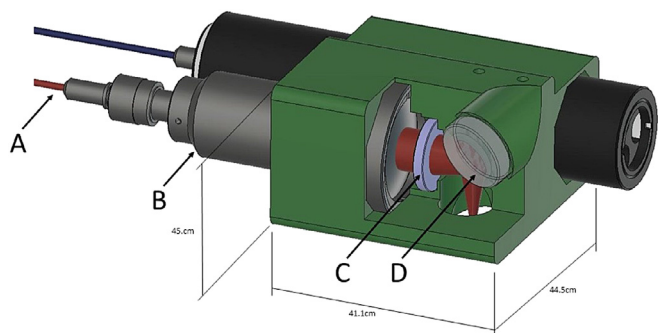


Fig. 4. Section view of the optics assembly showing LIBS laser delivery optics. The laser is delivered through the red fiber (A), collimated (B), focused (C), and reflected (D) towards the target surface. The laser is represented by a red beam path through the optics. (For interpretation of the references to colour in this figure legend, the reader is referred to the Web version of this article.)

laser repetition rate of 10 Hz. The beam is focused by a 200-mm plano-convex lens (Thorlabs LA1708-YAG) onto a cleaved fiber tip in order to couple the beam into the 1-mm core diameter fiber (Thorlabs FT1000EMT). This fiber is then added to the main PRINSE cable bundle and routed to the robotic delivery train. Inside the LIBS train car, the fiber is terminated with an air-spaced double lens collimator (Thorlabs F810SMA-1064), and the beam is then focused with a plane-convex lens (Newport KPX043AR.33) and redirected with a 45° laser line mirror (Edmund Optics 45–986) towards the target surface, as shown in Fig. 4. The lens and mirror coatings along the laser delivery optical path were chosen to maximize the transmission at the LIBS excitation laser wavelength (1064 nm). The use of three DP sequences ensures that all chlorine is removed from the surface at the target location (Xiao et al., 2018).

The efficacy of excitation of chlorine emission is dependent on the laser intensity produced on the canister surface, which requires maximization of the delivered peak power for a given laser spot size. The peak power delivered to the canister surface is limited by several factors, including optical damage at the optical fiber input, coupling efficiency into the fiber, attenuation during propagation through fiber and final LIBS optics, and temporal broadening of the laser pulse due to the multimodal dispersion in the fiber. The temporal broadening of the laser pulse after propagation through the 25-m long, 1-mm core diameter fiber was measured to be 7.3%, (from 15.0 ns to 16.1 ns). We experimentally determined that the maximum laser intensity produced on the canister surface when using this optical system was sufficient for excitation of the desired chlorine line. Optical damage at the fiber input was mitigated through fine adjustments of laser coupling and visual inspection of the quality of the fiber cleaved surface during tip preparation.

Due to the use of a class 4 laser, safety precautions were necessary. In order to improve safety while working in the field, the fiber coupling optics were enclosed in a light-tight box. This removes the requirement for eye protection for the operator and personnel in the area once the laser-fiber coupling procedures have been completed. Upon arrival to the operation site, the operator should verify the coupling efficiency and make adjustments as required. During this time, eye protection is required, since the enclosure has to be temporarily opened. The laser head includes two mechanical shutters that need to be opened by the operator. As a standard operating procedure, the shutters should only be opened either under controlled test conditions or once the PRINSE train has been inserted into the channel and measurements are to begin.

3.1.2. Collection of plasma emission

Once the plasma is formed, the plume expands away from the ablation site on the canister surface. A fraction of the light emitted by the plasma is collected and collimated by an off-axis parabolic mirror

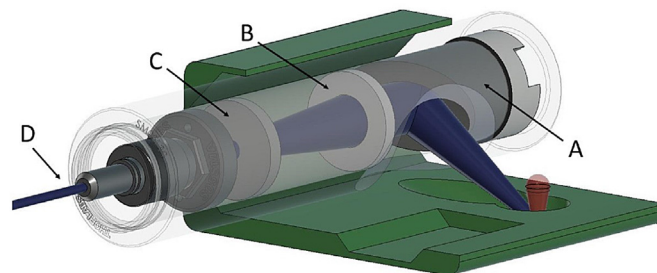


Fig. 5. Section view of the optics assembly showing the LIBS collection optics. A portion of the plasma emission is collimated by a parabolic mirror (A), focused (B), filtered (C), and coupled into a 25-m long optical fiber (D) for transport to the LIBS external module. The path of the incident laser pulse is represented by the red cone, while the collected solid angle from plasma emission is represented by the blue beam path. (For interpretation of the references to colour in this figure legend, the reader is referred to the Web version of this article.)

(Thorlabs MPD019-M01), focused with a 30-mm plano-convex lens (THORLABS LA1289-B), and passed through a high-pass filter (Newport 5CGA-550), after which it is coupled into the second optical fiber. All of the aforementioned optics are secured inside a standard lens tube with an access hole drilled orthogonally, allowing light from the plasma emission to reach the parabolic mirror, as depicted in Fig. 5. To help maintain proper distances between the optical components, aluminum sleeves are cut to the designed distances. Once coupled to the collection tube, the fiber is routed through the same main bundle back to the external LIBS module and terminated at the entrance to the spectrometer (Horiba iHR550). The spectrometer is equipped with a set of three diffraction gratings (1200, 2400, and 3600 lines/mm). The plasma emission spectrum is digitized by an ICCD detector (Andor DH334T-18F-03) and processed using a real-time virtual instrument implemented in the LabView framework.

The spectral line chosen for detection is the neutral Cl I 837.6-nm line (Xiao et al., 2018). We chose a 3600 lines/mm grating for our measurement. This grating provides a spectral window of 15.6 nm and a good spectral resolution that enables a clear observation of the two prominent iron (Fe I) lines (832.7 nm and 838.6 nm) in the vicinity of the selected Cl I line. The two intense characteristic peaks from iron are used to validate and optimize the system operation. They serve as a relative reference when measuring the chlorine concentration on the surface.

Antireflective coatings were chosen to minimize the attenuation of the 837.6-nm emission as it is transported through the optical system, from its origin in the plasma plume to the ICCD. Other species present in the plasma (such as iron) emit characteristic lines at wavelengths that may cause multi-order interference once diffracted by the spectrometer grating. In order to remove such interferences, a high-pass filter with a cutoff wavelength of 550 nm is used inside the optics holder.

Due to the spatial constraints, a parabolic mirror was chosen to efficiently collect and collimate plasma emission. The shortest of-the-shelf focal length available of 25.4-mm diameter was used, which results in a relatively small depth of focus (~1 mm), and thus a limited field of view for the collection system. Due to the angle between the motion of the expanding plasma and the optical path, the image created by the optics sweeps across the fiber tip as the plasma expands. This, in turn, results in a limited time period over which the characteristic emission from the rapidly expanding plasma can be efficiently collected. An attempt to increase the light collected from this sweeping motion was made by introducing a cosine corrector diffuser, which homogenizes the light for more consistent coupling into fiber. However, this resulted in an unacceptably high loss of efficiency when coupling to the fiber. Because the collection optics are placed at an off-axis angle

with respect to the principal direction of plume expansion, the combination of the angle at which the plasma is viewed, the ICCD detector delay, and integration time become interdependent and need to be carefully adjusted and calibrated.

3.2. Material considerations

The harsh environment inherent to the PRINSE concept of operations requires the design to take into account temperature induced changes to material and radiation effects, such as darkening of the optical fiber. Under normal operating conditions, the PRINSE robotic train is subject to irradiation from both gamma rays and neutrons (Priest, 2016). Also, the PEEK (polyether ether ketone) material was selected for all non-optical components so that additive manufacturing can be used to rapidly prototype the optics holder. Also, PEEK is relatively resistant to radiation damage in comparison to other polymers that are also compatible with operation at elevated temperatures expected in the dry cask storage environment (Yoda, 1984).

3.2.1. System integration

To quantify concentration, the LIBS measurement makes the assumption of complete removal of salt from the stainless steel surface and no overlapping measurements when multiple spots are studied. We have previously studied the characteristics of the stainless steel surface after the incidence of the laser pulse to determine the diameter of the heat affected zone (Xiao et al., 2017), which was found to be approximately 1 mm. We use 2.5 mm as the minimum distance required between the neighboring spots measured by LIBS such that the chlorine concentration is not affected by prior neighboring measurements.

The PRINSE positioning system provides an electronic signal, indicating that the motion of the car has exceeded the minimum distance of 1 mm. Once this signal has been received through the PRINSE control system, the LabView VI sends a command to the ICCD detector to commence data acquisition. The ICCD's built-in digital delay generator further sends a logic signal that triggers the generation of the laser pulse. Three DP sequences per location on the surface are accumulated within the ICCD data acquisition system and sent to the LabView VI. The data is logged locally in ASCII format, with each record consisting of a 1024-element array of data points representing the acquired spectrum. In addition, an automated real-time chlorine concentration analysis is performed by use of previously measured calibration curves and the results are displayed to the operator (Fig. 6). In order to construct calibration curves, spectral line intensities are quantified (Xiao et al., 2018) for each chlorine concentration. Once data collection is complete, a message is sent over the PRINSE network, which logs the event time and location along the canister.

It is necessary for the LIBS final optics to establish the optimal distance to the surface and maintain it during operation to ensure consistency in laser focusing on the surface and in the collection of optical emission from the plasma. To meet this requirement, the optics holder was designed such that the base of the holder makes contact with the target surface. The final optics holder is allowed to pivot inside the train car and is retracted from the target surface by a set of springs when not in operation. During sampling, a pneumatic actuator provides pressure for the holder to make a contact with the target, as shown in Fig. 7. The choice of pneumatic actuation reduces the use of electronics inside the train car, increasing its robustness.

A side benefit resulting from meeting the spatial constraints of the robotic train is the reduction of risk for damage to expensive equipment from normal operation. By remotely operating the laser, ICCD and spectrometer the risk of damage from heat and radiation are easily managed by the operator. In the event that the optics become activated by the radioactive environment, their replacement cost is low compared to the replacement cost of other system components.

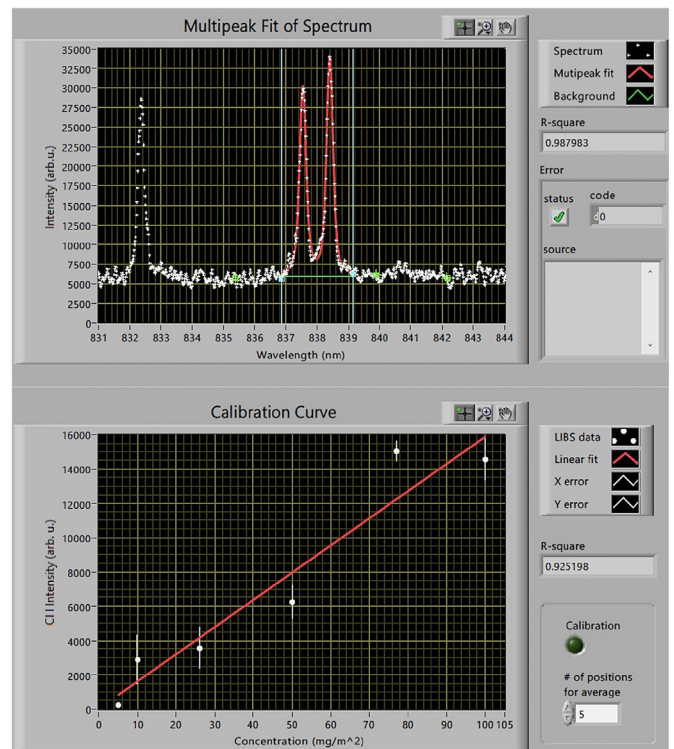


Fig. 6. Section of the LabView interface designed for real-time data processing and feedback.



Fig. 7. The LIBS optics holder mounted in the PRINSE train car. Operation of this system was tested once fully inserted into a simulated canister channel.

3.2.2. Fiber management

The fiber optic cable chosen for this application allows for a bend radius as low as 5 cm, but as with many applications that involve the use of optical fibers, twisting the cable is not possible. In order to safely handle the cable bundle and prevent its damage, the PRINSE bundle is laid out near the insertion channel and manually assisted as the train is lowered. Additionally, the cable bundle is placed into a sheath to further prevent damage. This sheath provides the second safety barrier to the optical hazard. In the event the fiber is damaged between the operator cart and the LIBS car, the sheath will both absorb and diffuse the

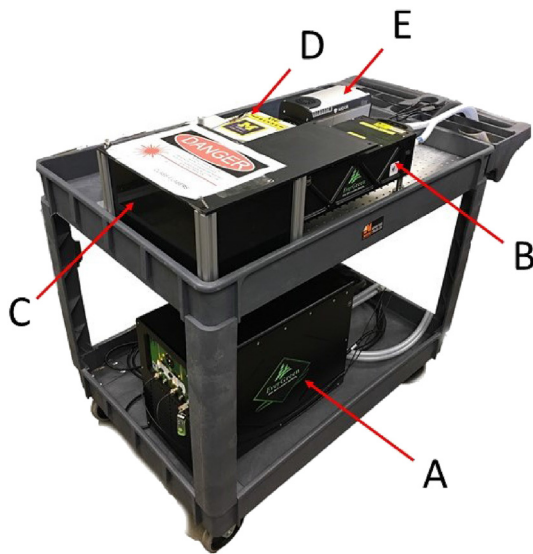


Fig. 8. The external LIBS module is designed to fit onto a single cart, which contains the laser power supply (A), DP laser head (B), fiber launch enclosure (C), spectrometer (D), and ICCD detector (E).

laser energy, mitigating any laser eye hazard.

3.2.3. Deployable field cart

To ease of operation in the field, we designed an arrangement that allows for the external LIBS module to be placed on a single cart. However, due to the nature of the components used (laser, spectrometer, and ICCD), which are designed for operation in a controlled laboratory environment, environmental conditions must be considered. The use of air conditioning at near-room temperature and with low humidity and minimum temperature fluctuation is recommended for these components.

As shown in Fig. 8, the cart holds the laser power supply, laser head, enclosed laser/fiber coupling optics, spectrometer, and ICCD. The cart further holds an uninterruptible power supply, with entire system being powered by one 110-V power cord. A single USB cable interfaces the cart to the operator's computer. A Cat5-standard cable is used to transmit the PRINSE LIBS signal to the cart, and two optical fibers are routed from the cart to the train car. As there are only three fine optical adjustments needed (two for laser/fiber coupling, and the collection tube), the PRINSE LIBS system can be rapidly deployed to make measurements in the field.

4. Design verification

The performance of the PRINSE LIBS system was evaluated in two distinct environments. First, we tested the operation in a research laboratory with stainless steel samples that were prepared to contain known chlorine concentrations. Next, we conducted experiments in a simulated field environment, where the complete integration into the PRINSE system was explored.

4.1. Spectroscopic performance

The spectroscopic components of the PRINSE LIBS subsystem were tested using the same procedures previously employed in our proof-of-principle studies of chlorine detection (Xiao et al., 2018). The final optics holder was allowed to rest against the target surface, mimicking the geometry that would be experienced in the field. Fig. 9 demonstrates the performance improvements realized between feasibility measurements taken on a laboratory bench optical setup and measurements made using the final optics assembly. The samples used in

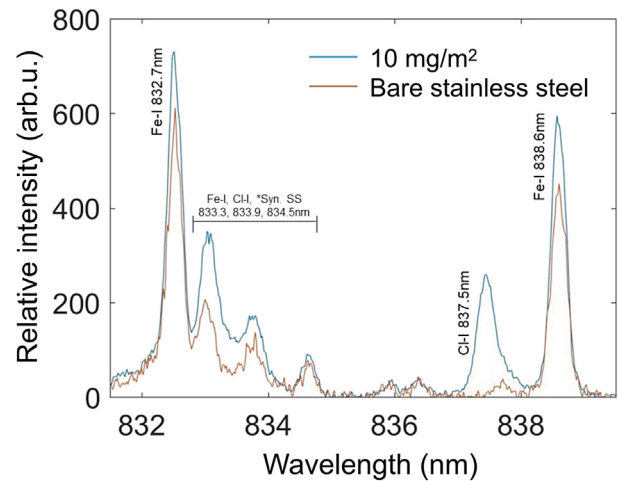


Fig. 9. Test results from the remote LIBS optics system while deployed in the robotic train, verifying a chlorine concentration of 10 mg/m² on stainless steel is observable. Also shown is the result from a sample which chlorine has been removed, in which the Cl I peak is not present. The triple peaks between 833.3 nm and 834.5 nm are a convolution of iron, chlorine, and other elements present in the synthetic sea salt.

both measurements had chlorine surface concentrations of 10 mg/m² of chlorine in the form of NaCl deposited on a stainless steel sample coupon.

The improvement in performance realized between the laboratory benchtop measurement and the simulated field measurement does not necessarily reflect the ultimate capability of the laboratory setup. Rather, the laboratory bench optical setup did not undergo the lengthy experimentation that was conducted to optimize the performance of the PRINSE LIBS optics holder used in field measurements. However, the final result from integrated tests shows that, despite the challenges to meet all design constraints, detection of chlorine at low concentrations is possible with this design.

4.2. System integration

The LIBS components were fully integrated into the PRINSE system for a technology demonstration, which was conducted on a dry cask storage mock-up setup constructed at the Penn State University's Test Track Facility. The mock-up was built using the specifications of the Holtec HI-STORM 100, including the curved surface that must be accounted for in the optical design. The test site allowed for an air-conditioned environment for the LIBS equipment. The demonstration culminated with insertion of the entire robotic train into a simulated dry cask storage channel and down the full length of the canister wall. At the base of the canister, movement of the fiber optic cables was verified, demonstrating that it was possible to negotiate the maneuvers required for insertion without damaging the fiber cables. Additionally, during the demonstration, communication over the PRINSE network provided accurate vertical position of the LIBS car as well as an acknowledgement of the receipt of the sample signal. This signal is an additional safety measure to ensure that the laser will not be operated under unsafe conditions that are outside of the LIBS subsystem control. As the PRINSE train traverses the canister surface, the LIBS system samples for chlorine at discrete distance intervals, with a minimum of 2.5 mm of travel to ensure non-interfering sample locations.

5. Conclusion

We have developed a portable laser-based inspection system and demonstrated the use of DP excitation technique to improve the analytical performance of fiber optic-based LIBS in detection. Laser

excitation and detection systems were effectively separated to a 25-m distance, as measured from the external LIBS assembly to LIBS final optics. Two multimode optical fibers were used as interface between those two system components; one optical fiber was used for laser delivery, while the other guided the collected plasma emission to the spectrometer. Propagation through an optical fiber of this length resulted in a relatively small change of the laser pulse parameters; it is therefore possible to further increase the distance to the final optics module as necessary. The challenges associated with coupling of the laser pulse into the optical fiber and collecting the plasma emission were addressed in the design. The limited space for laser delivery within the robotic train was addressed by constructing a custom, 3D-printed holder, and by using compact (12.5-mm) diameter optics. The optical fiber characteristics allow sufficient flexibility for the fiber to be inserted through the dry cask storage air vent while bending as long as the radii are greater than the minimum 5-cm bend radius.

Even though the system was designed to be as robust as possible, it employs commercial off-the-shelf components intended primarily for operation in scientific laboratory conditions. Consequently, care is needed when transporting the sensitive equipment to the measurement location to avoid damage. For example, it is advised to avoid temperature gradients and prevent exposure to excessive humidity, that could lead to condensation and failure of optical components exposed to high-power laser beam. Finally, the compact DP LIBS setup was effectively integrated into a multi-sensor PRINSE system, which has been proven capable of detecting chlorine concentrations down to 10 mg/m² on a stainless steel surface. The DP LIBS measurement configuration presented in this paper provides a viable guide to significantly improve the functionality and applicability of field-deployable LIBS technology. Furthermore, the same operating principles of this system could in principle be adapted for other applications such as remote repair and mitigation of cracks by means of laser welding.

Acknowledgments

We would like to thank Patrick Skrodzki and Kyle Hartig for their help with the development of the LIBS setup, and Ian Van Sant, Sean Brennan, Cliff Lissenden, Mike Zuger, and Karl Reichard for their assistance of the LIBS integration into the PRINSE multi-sensor system. This work was supported by the Department of Energy Nuclear Energy University Program under Integrated Research Project award number DE-NE0008266.

References

- Babushok, V.I., DeLucia, F.C., Gottfried, J.L., Munson, C.A., Miziolek, A.W., 2006. Double pulse laser ablation and plasma: laser induced breakdown spectroscopy signal enhancement. *Spectrochim. Acta B Atom Spectrosc.* 61 (9), 999–1014. <https://doi.org/10.1016/j.sab.2006.09.003>.
- Benedetti, P.A., Cristoforetti, G., Legnaioli, S., Palleschi, V., Pardini, L., Salvetti, A., Tognoni, E., 2005. Effect of laser pulse energies in laser induced breakdown spectroscopy in double-pulse configuration. *Spectrochim. Acta B Atom Spectrosc.* 60 (11), 1392–1401. <https://doi.org/10.1016/j.sab.2005.08.007>.
- Bryan, C.R., Enos, D.G., 2015. SNF Interim Storage Canister Corrosion and Surface Environment Investigations. Technical Report FCRD-UFD-2013-000324. Sandia National Laboratories (SNL-NM), Albuquerque, NM (United States).
- Burakov, V.S., Kiris, V.V., Raikov, S.N., 2007. Optimization of conditions for spectral determination of chlorine content in cement-based materials. *J. Appl. Spectrosc.* 74 (3), 321–327. <https://doi.org/10.1007/s10812-007-0052-5>.
- Chu, S., 2013. Failure Modes and Effects Analysis (FMEA) of Welded Stainless Steel Canisters for Dry Cask Storage Systems. Electric Power Research Institute Report 3002000815.
- Cremers, D.A., Radziemski, L.J., 2013. *Handbook of Laser-Induced Breakdown Spectroscopy*. Wiley ISBN 9781118567340.
- Cremers, D.A., Barefield, J.E., Koskelo, A.C., 1995. Remote elemental analysis by laser-induced breakdown spectroscopy using a fiber-optic cable. *Appl. Spectrosc.* 49 (6), 857–860. <https://doi.org/10.1366/0003702953964589>.
- Hahn, David W., Omenetto, Nicoló, 2010. Laser-induced breakdown spectroscopy (libs), part i: review of basic diagnostics and plasma—particle interactions: still-challenging issues within the analytical plasma community. *Appl. Spectrosc.* 64 (12), 335A–336A. <https://doi.org/10.1366/000370210793561691>.
- Davies, C.M., Telle, H.H., Montgomery, D.J., Corbett, R.E., 1995. Quantitative analysis

- using remote laser-induced breakdown spectroscopy (libs). *Spectrochim. Acta B Atom Spectrosc.* 50 (9), 1059–1075. [https://doi.org/10.1016/0584-8547\(95\)01314-5](https://doi.org/10.1016/0584-8547(95)01314-5).
- Eto, Shuzo, Fujii, Takashi, 2016. Laser-induced breakdown spectroscopy system for remote measurement of salt in a narrow gap. *Spectrochim. Acta B Atom Spectrosc.* 116 (Suppl. C), 51–57. <https://doi.org/10.1016/j.sab.2015.12.003>.
- Gehlen, C.D., Wiens, E., Noll, R., Wilsch, G., Reichling, K., 2009. Chlorine detection in cement with laser-induced breakdown spectroscopy in the infrared and ultraviolet spectral range. *Spectrochim. Acta B Atom Spectrosc.* 64 (10), 1135–1140. <https://doi.org/10.1016/j.sab.2009.07.021>.
- Girard, S., Kuhnemann, J., Gusarov, A., Brichard, B., Van Uffelen, M., Ouerdane, Y., Boukenter, A., Marcandella, C., 2013. Radiation effects on silica-based optical fibers: recent advances and future challenges. *IEEE Trans. Nucl. Sci.* 60 (3), 2015–2036. <https://doi.org/10.1109/TNS.2012.2235464>.
- Gornushkin, I.B., Anzano, J.M., King, L.A., Smith, B.W., Omenetto, N., Winefordner, J.D., 1999. Curve of growth methodology applied to laser-induced plasma emission spectroscopy. *Spectrochim. Acta B Atom Spectrosc.* 54 (3), 491–503. [https://doi.org/10.1016/S0584-8547\(99\)00004-X](https://doi.org/10.1016/S0584-8547(99)00004-X).
- Kramida, A., Ralchenko, Y., Reader, J., 2017. Nist Atomic Spectra Database. National Institute of Standards and Technology, Gaithersburg, MD. <http://physics.nist.gov/asd>.
- Labutin, T.A., Popov, A.M., Raikov, S.N., Zaytsev, S.M., Labutina, N.A., Zorov, N.B., 2013. Determination of chlorine in concrete by laser-induced breakdown spectroscopy in air. *J. Appl. Spectrosc.* 80 (3), 315–318. <https://doi.org/10.1007/s10812-013-9766-8>.
- Labutin, T.A., Popov, A.M., Zaytsev, S.M., Zorov, N.B., Belkov, M.V., Kiris, V.V., Raikov, S.N., 2014. Determination of chlorine, sulfur and carbon in reinforced concrete structures by double-pulse laser-induced breakdown spectroscopy. *Spectrochim. Acta B Atom Spectrosc.* 99 (1), 94–100. <https://doi.org/10.1016/j.sab.2014.06.021>.
- Li, Shuo, Liu, Lei, Yan, Aidong, Huang, Sheng, Huang, Xi, Chen, Rongzhang, Lu, Yongfeng, Chen, Kevin, 2017. A compact field-portable double-pulse laser system to enhance laser induced breakdown spectroscopy. *Rev. Sci. Instrum.* 88 (2). <https://doi.org/10.1063/1.4975597>. 023109.
- Lissenden, C.J., Choi, S., Cho, H., Motta, A., Hartig, K., Xiao, X., Le Berre, S., Brennan, S., Reichard, K., Leary, R., McNelly, B., Jovanovic, I., 2016. Toward robotic inspection of dry storage casks for spent nuclear fuel. *J. Pressure Vessel Technol.* 139 (3). <https://doi.org/10.1115/1.4035788>. 031602.
- Miziolek, A.W., Palleschi, V., Schechter, I., 2006. *Laser Induced Breakdown Spectroscopy*. Cambridge University Press ISBN 9781139458313.
- Nagasawa, K., Tanabe, M., Yahagi, K., 1984. Gamma-ray-induced absorption bands in pure-silica-core fibers. *Jpn. J. Appl. Phys.* 23 (12R), 1608. <https://doi.org/10.1143/JJAP.23.1608>.
- Neuhauser, R.E., Panne, U., Niessner, R., 2000. Utilization of fiber optics for remote sensing by laser-induced plasma spectroscopy (lips). *Appl. Spectrosc.* 54 (6), 923–927. <https://doi.org/10.1366/0003702001950337>.
- Noll, R., 2012. *Laser-Induced Breakdown Spectroscopy: Fundamentals and Applications*. Springer Berlin Heidelberg ISBN 9783642206689.
- Pedarnig, J.D., Haslinger, M.J., MA, Bodea, Huber, N., Wolfmeir, H., Heitz, J., 2014. Sensitive detection of chlorine in iron oxide by single pulse and dual pulse laser-induced breakdown spectroscopy. *Spectrochim. Acta B Atom Spectrosc.* 101, 183–190. <https://doi.org/10.1016/j.sab.2014.08.028>.
- Priest, C.R., 2016. Dosimetry, Activation, and Robotic Instrumentation Damage Modeling of the Holtec Hi-storm 100 Spent Nuclear Fuel System. Master's thesis. University of South Carolina.
- Rai, A.K., Zhang, H., Yueh, F.Y., Singh, J.P., Weisberg, A., 2001. Parametric study of a fiber-optic laser-induced breakdown spectroscopy probe for analysis of aluminum alloys. *Spectrochim. Acta B Atom Spectrosc.* 56 (12), 2371–2383. [https://doi.org/10.1016/S0584-8547\(01\)00299-3](https://doi.org/10.1016/S0584-8547(01)00299-3).
- Saeki, M., Iwanade, A., Ito, C., Wakaida, I., Thornton, B., Sakka, T., Ohba, H., 2014. Development of a fiber-coupled laser-induced breakdown spectroscopy instrument for analysis of underwater debris in a nuclear reactor core. *J. Nucl. Sci. Technol.* 51 (7–8), 930–938. <https://doi.org/10.1080/00223131.2014.917996>.
- Sugiyama, K., Fujii, T., Matsumura, T., Shiogama, Y., Yamaguchi, M., Nemoto, K., 2010. Detection of chlorine with concentration of 0.18 kg/m³ in concrete by laser-induced breakdown spectroscopy. *Appl. Opt.* 49 (13), C181–C190. <https://doi.org/10.1364/AO.49.00C181>.
- Tran, Michael, Sun, Qing, Smith, Benjamin W., Winefordner, James D., 2001. Determination of F, Cl, and Br in solid organic compounds by laser-induced plasma spectroscopy. *Appl. Spectrosc.* 55 (6), 739–744. <https://doi.org/10.1366/0003702011952433>.
- Whitehouse, A.I., Young, J., Botheroyd, I.M., Lawson, S., Evans, C.P., Wright, J., 2001. Remote material analysis of nuclear power station steam generator tubes by laser-induced breakdown spectroscopy. *Spectrochim. Acta B Atom Spectrosc.* 56 (6), 821–830. [https://doi.org/10.1016/S0584-8547\(01\)00232-4](https://doi.org/10.1016/S0584-8547(01)00232-4).
- Wilsch, G., Weritz, F., Schaurich, D., Wiggerhauser, H., 2005. Determination of chloride content in concrete structures with laser-induced breakdown spectroscopy. *Construct. Build. Mater.* 19 (10), 724–730. <https://doi.org/10.1016/j.conbuildmat.2005.06.001>.
- Xiao, X., Le Berre, S., Hartig, K.C., Motta, A.T., Jovanovic, I., 2017. Surrogate measurement of chlorine concentration on steel surfaces by alkali element detection via laser-induced breakdown spectroscopy. *Spectrochim. Acta B Atom Spectrosc.* 130, 67–74. <https://doi.org/10.1016/j.sab.2017.02.011>.
- Xiao, X., Le Berre, S., Fobar, D.G., Burger, M., Skrodzki, P.J., Hartig, K.C., Motta, A.T., Jovanovic, I., 2018. Measurement of chlorine concentration on steel surfaces via fiber-optic laser-induced breakdown spectroscopy in double-pulse configuration. *Spectrochim. Acta B Atom Spectrosc.* 141, 44–52. <https://doi.org/10.1016/j.sab.2018.01.003>.
- Yoda, O., 1984. The radiation effect on non-crystalline poly(aryl-ether-ketone) as revealed by x-ray diffraction and thermal analysis. *Polym. Commun.* 25, 238–240.